
Mogao: An Omni Foundation Model for Interleaved Multi-Modal Generation

Chao Liao*, Liyang Liu*, Xun Wang*, Zhengxiong Luo*, Xinyu Zhang, Wenliang Zhao, Jie Wu, Liang Li, Zhi Tian[†], Weilin Huang[‡]

ByteDance Seed

*Equal Contribution, [†]Project Lead, [‡]Corresponding authors

Abstract

Recent progress in unified models for image understanding and generation has been impressive, yet most approaches remain limited to single-modal generation conditioned on multiple modalities. In this paper, we present Mogao, a unified framework that advances this paradigm by enabling interleaved multi-modal generation through a causal approach. Mogao integrates a set of key technical improvements in architecture design, including a deep-fusion design, dual vision encoders, interleaved rotary position embeddings, and multi-modal classifier-free guidance, which allow it to harness the strengths of both autoregressive models for text generation and diffusion models for high-quality image synthesis. These practical improvements also make Mogao particularly effective to process interleaved sequences of text and images arbitrarily. To further unlock the potential of unified models, we introduce an efficient training strategy on a large-scale, in-house dataset specifically curated for joint text and image generation. Extensive experiments show that Mogao not only achieves state-of-the-art performance in multi-modal understanding and text-to-image generation, but also excels in producing high-quality, coherent interleaved outputs. Its emergent capabilities in zero-shot image editing and compositional generation highlight Mogao as a practical omni-modal foundation model, paving the way for future development and scaling the unified multi-modal systems.

Date: May 13, 2025



Figure 1 Mogao Text-to-Image visualization.



Figure 2 Mogao Interleaved Multi-Modal Generation Visualization.

1 Introduction

Generative models have shown significant potential to advance towards artificial general intelligence (AGI). Contemporary models, such as large language models (LLMs) [7, 77] and text-to-image (T2I) models [20, 25, 32, 69, 80], typically process single-modal inputs and generate single-modal outputs. However, to interact with users in a human-like manner, models must be capable of interpreting arbitrarily interleaved multi-modal inputs and generating corresponding multi-modal outputs. Such models can seamlessly integrate multiple modalities, as illustrated in Fig. 2, to convey meaningful and more accurate information through a combination of text and visuals.

Early efforts in unified multi-modal modeling have leveraged auto-regressive (AR) models for text generation. By introducing visual tokenizers and de-tokenizers, image patches can be processed as text tokens, facilitating the seamless extension of traditional LLMs to large multi-modal models. These models have demonstrated excellent performance in visual understanding [4, 58]. However, AR-based approaches for image generation often encounter limitations, including low training efficiency [92], exposure bias [26], and suboptimal image tokenization [39]. Inspired by the success of diffusion-based models in visual generation [28, 32], recent research has explored hybrid AR-diffusion architectures to advance unified multi-modal modeling. For instance, Transfusion [96] integrates an AR model and a diffusion model by sharing transformer weights, enabling text generation via next-token prediction and image generation via iterative denoising. While these approaches leverage the strengths of both paradigms, the implications of shared weights remain underexplored.

In this work, we develop a practically efficient hybrid architecture that seamlessly integrates AR-based text generation with diffusion-based image generation. Text tokens and image embeddings are combined into a unified input sequence, processed by a transformer equipped with modality-specific QKV and FFN layers, diverging from modality-shared designs. We introduce a novel position embedding scheme that assigns distinct modality-specific IDs and frequency patterns. Supervision is applied separately: next-token prediction loss for text and diffusion loss for images. To disentangle understanding and generation tasks, we decouple the Multi-Layer Perceptron (MLP) parameters within the transformer and employ different image encoders—such as a Vision Transformer (ViT) for understanding and a Variational Autoencoder (VAE) for generation. This separation mitigates task interference, enhancing performance across both domains.

In contrast to conventional unified models that depend heavily on paired data supervision, our approach allows **Mogao**¹ to pioneer native interleaved multi-modal modeling. To facilitate this, we construct a ten-million-scale interleaved multi-modal dataset. Additionally, we design a compute-efficient training strategy that simultaneously optimizes teacher-forced textual tokens and diffusion-based corrupted visual tokens within interleaved sequences. A central innovation lies in our multi-conditioned image generation paradigm: unlike traditional models constrained to single-modal inputs (e.g., text-to-image), our method dynamically incorporates contextual information from both preceding text and images. Moreover, a standard classifier-free guidance (CFG) approach risks image repetition during interleaved generation due to varying transferability between intra- and cross-modal tokens. To mitigate this, we introduce a dual CFG mechanism that integrates both empty and visual-only conditions, thereby enhancing the precision of image generation.

The primary contributions of **Mogao** encompass the following three aspects:

- We propose a conceptually elegant and highly effective unified architecture that seamlessly integrates autoregressive and diffusion models, enabling superior both text and image generation.
- We introduce a suite of innovative technical improvements that facilitate efficient training and inference for interleaved multi-modal understanding and generation.
- We conduct comprehensive experiments, including ablation studies, to rigorously validate our approach, achieving state-of-the-art performance across multiple open benchmarks, substantiated by human evaluations for multi-modal generation.

¹The Mogao Caves are the best known of the Chinese Buddhist grottoes, which contain some of the finest examples of Buddhist art spanning a period of 1,000 years.

2 Related Work

Visual understanding and generation have traditionally been handled by separate models: vision language models [49, 50] for understanding and diffusion models [20, 25, 28, 69] for generation. Recently, efforts to unify the two tasks into a single foundation model have gained momentum, driven by the potential to produce higher quality, more consistent multimodal content [2, 85].

Unified Framework A central challenge in building unified models is the misalignment between text and visual modalities. State-of-the-art vision-language models (VLMs) are typically built on GPT-style large language models (LLMs) [7, 63, 64], and trained via next-token prediction [4, 35, 81]. In contrast, high-performance visual generation models are based on diffusion models [18, 32]. Recent efforts attempted to unify visual generation within an auto-regressive (AR) framework by using next-token prediction. For example, the Emu series [72, 73] consider images as continuous feature vectors concatenated with text embeddings, allowing a language model [77] to generate both text tokens and image vectors autoregressively. Similarly, Chameleon [74] replaces continuous image features with discrete visual tokens. However, AR methods often struggle to generate high-quality images [8, 39, 75], compared to diffusion-based approaches.

Other approaches embed diffusion modules directly into an LLM backbone. For example, recent approaches such as Show-O [88] and TransFusion [96], are able to generate text token-by-token, and synthesize an images through a diffusion process, by sharing a transformer backbone [60, 78]. This can improve the performance of visual generation, but might sacrifice the understanding capability, due to the conflicts of two tasks learning with shared parameters [44, 45]. In **Mogao**, we adopt the MMDiT architecture [18], which decouples two tasks by using separate text and visual parameters to reduce such cross-modal conflicts.

Unified Representation Another challenge lies in the differing requirements of visual representations for understanding and generation [55, 62]. Features optimized for understanding may be suboptimal for generation, making visual tokenizer design critical. For example, SEED [21, 22] supervises its tokenizer using a reconstruction loss for generation while aligning tokenized features with CLIP for understanding [65]. Recent methods [55, 86] adopt a similar strategy, aligning the latent space of VQGAN [17] or VAE [31, 69] with semantic encoders [59, 95]. Although this improves overall performance, it still involves trade-offs between understanding and generation. JanusFlow [56] mitigates this by employing separate tokenizers: SigLIP [95] for understanding and a VAE for generation, enhancing both tasks simultaneously.

Interleaved Multi-Modal Generation A key application of omni-foundation models is interleaved multi-modal generation. Prior work [72, 91] shows that AR models trained on interleaved data can generate both text and images conditioned on mixed modalities, enabling unified capabilities such as image understanding, text-to-image generation, image editing, and composition. Further developments [87, 96] enhance visual fidelity by replacing token-wise synthesis with diffusion-based iterative denoising. However, these models typically focus on single-turn outputs, generating either text or image in isolation. In **Mogao**, we extend this to multi-turn interleaved generation.

3 Mogao

Vision Language Models (VLMs) [50, 54, 81] perform visual understanding by modeling the conditional distribution $P(\mathbf{x}_{\text{txt}} \mid \mathbf{x}_{\text{img}}, \mathbf{x}_{\text{txt}})$, while Text-to-Image (T2I) models [18, 32] perform image generation using $P(\mathbf{x}_{\text{img}} \mid \mathbf{x}_{\text{txt}})$. **Mogao** uses a unified backbone to model the joint distributions of images and text, naturally possessing the ability of both understanding and image generation. In addition, in this paper, we extend its generative capabilities by using a causal approach, which enables **Mogao** to implement a more complicated task: interleaved multi-modal generation, whereby using any modalities information generated in the past as a condition to generate new outputs in any modalities.

Multi-Modal Understanding Text data can be represented by the discrete token sequence $\mathbf{z} = (z_0, \dots, z_L)$, and LLMs model its joint distribution in a causal manner. Based on LLM, VLM converts visual features into

continuous token sequences by integrating visual encoders [65, 95] to process visual input. By training on large-scale multi-modal datasets, VLM expands the conditional distribution:

$$\log P_{\theta_{\text{VLM}}}(\mathbf{z} | \mathbf{x}) = \sum_{l=0}^L \log P_{\theta_{\text{VLM}}}(z_{l+1} | z_0, \dots, z_l, \mathbf{x}) \quad (1)$$

Where θ_{VLM} and $\mathbf{x} = (x_0, \dots, x_N)$ denote the parameters of VLM and the continuous token sequence of visual input respectively, and \mathbf{x} can be \emptyset . In general, both LLMs and VLMs only output text tokens z_i . Therefore, we can optimize the model by minimizing the cross-entropy between P_θ and the data distribution, which is the so-called next token prediction (NTP) loss:

$$\mathcal{L}_{\text{NTP}} = \mathbb{E}_{z_i} [-\log P_{\theta_{\text{VLM}}}(z_{l+1} | z_0, \dots, z_l, \mathbf{x})] \quad (2)$$

Visual Generation In this paper, we adopt rectified flow matching [51] to model image distribution, which is simple in concept but performs well in text-to-image generation [18]. Given the image distribution $\mathbf{x} \sim \pi$ and a simple prior distribution $\epsilon \sim \mathcal{N}(0, 1)$, we construct a linear trajectory defined over time t :

$$\mathbf{x}_t = t \cdot \mathbf{x} + (1 - t) \cdot \epsilon, \quad t \in [0, 1] \quad (3)$$

The following ordinary differential equation (ODE) can be derived from Eq. (3):

$$\frac{d\mathbf{x}_t}{dt} = \mathbf{v}(\mathbf{x}_t, t) \quad (4)$$

where the velocity field $\mathbf{v} = \mathbf{x} - \epsilon$. To generate an image, we can perform the reverse time integration of ODE in Eq. (4) starting from $\mathbf{x}_0 \sim \mathcal{N}(0, 1)$, specifically, $\mathbf{x}_1 = \int_0^1 \mathbf{v}(\mathbf{x}_t, t) dt$. Therefore, for image generation, we need to train the network parameterized by θ to approximate \mathbf{v} by optimizing the flow matching loss:

$$\mathcal{L}_{\text{flow}} = \mathbb{E}_{t, \mathbf{x} \sim \pi, \epsilon \sim \mathcal{N}(0, 1)} \|\mathbf{v}_\theta(\mathbf{x}_t, t) - (\mathbf{x} - \epsilon)\|_2^2 \quad (5)$$

Interleaved Multi-Modal Generation In contrast to contemporary models which unify visual understanding and generation [56, 82, 88, 96], Mogao modeling the sequential distributions at the **modal level** in a causal manner:

$$\log P_\theta(\mathbf{x}) = \sum_{t=0}^T \log P_\theta(\mathbf{x}_{t+1} | \mathbf{x}_0, \dots, \mathbf{x}_t), \quad \mathbf{x}_t \in \{\mathbf{x}_{\text{img}}, \mathbf{x}_{\text{txt}}\} \quad (6)$$

Here, θ denotes the parameters of the model; notably, \mathbf{x}_t represents visual or text modality rather than an individual token. Once \mathbf{x}_{t+1} is generated, it will be added to the historical information as the condition. Thus, Mogao can facilitate the generation of any modality conditioned on an arbitrary mixture of modalities, to wit, interleaved multi-modal generation.

For the interleaved multi-modal generation task, we need to calculate the NTP loss in Eq. 2 for text and flow matching loss in Eq. 5 for noised image simultaneously in a sample of interleaved images and texts. Therefore, the overall training loss is a weighted combination of these two losses:

$$\mathcal{L}_{\text{total}} = \lambda \cdot \mathcal{L}_{\text{NTP}} + \mathcal{L}_{\text{flow}} \quad (7)$$

It is worth noting that during training, Mogao uses two special tokens to distinguish between visual and textual modalities. All image sequences will have the tokens $\langle |\text{vision_start}| \rangle$ and $\langle |\text{vision_end}| \rangle$ inserted at the

beginning and end, respectively. During inference, Mogao decides whether to generate an image based on the context. When generating `<|vision_start|>`, it switches to image generation mode, and when generating `<|vision_end|>`, it switches to text generation mode.

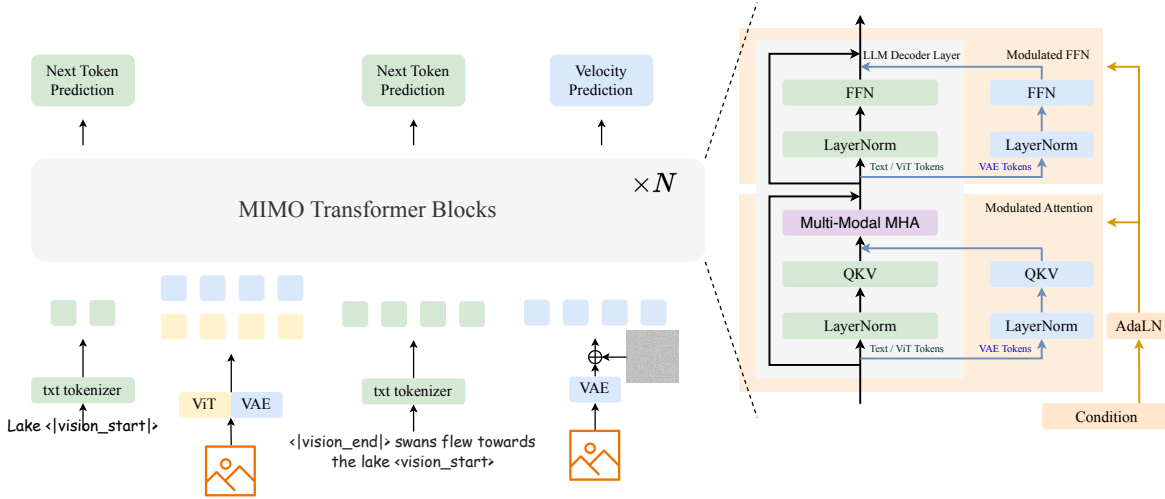


Figure 3 Overall framework of the proposed Mogao. The model consists of N modified LLM decoder layers, using different QKV matrix and FFN to process visual tokens. When the image is used as a condition, VAE and ViT are both used to extract visual features, and VAE is used alone when generating images. It is worth noting that we assign the same position id to the ViT token and its corresponding VAE token. The condition will modulate the visual token through an AdaLN layer.

3.1 Model

The detailed architecture of Mogao is illustrated in Fig. 3.

Improved Dual Visual Encoder for Interleaved Multi-Modal Generation For visual generation, current mainstream T2I models use the Variational Autoencoder (VAE) to encode images into a low-dimensional latent space before performing the diffusion process. However, we find that compared to the pre-aligned semantic visual representations obtained from ViT (e.g., SigLIP [95]) in VLM models, the visual representations produced by VAE are inadequate for visual understanding, which is also mentioned in works such as JanusFlow [56]. JanusFlow proposed utilizing a VAE as the visual encoder during visual generation (where images serve as the target distribution) while employing a ViT as the visual encoder during visual understanding (where images act as the condition).

In the context of Mogao’s interleaved multi-modal generation, we further refined this strategy. Specifically, when an image serves as a condition, Mogao simultaneously extracts both ViT and VAE visual representations and appends them into the historical sequence. For multi-modal understanding tasks, i.e., text token generation, text tokens will only attend to ViT tokens and text tokens in the historical sequence. Conversely, for multi-modal generation tasks, i.e., image generation, noisy VAE tokens attend to all tokens in the historical sequence, including ViT, VAE, and text tokens. Because visual representations from ViT can provide a robust semantic representation of images, facilitating improved contextual alignment for image generation.

Deep-Fusion Architecture Our model architecture is constructed upon a pre-trained large language model (LLM) and incorporates some design inspired by MMDiT [18] to enhance visual generation capabilities. Specifically, we employ Qwen2.5 [89] as the backbone and modify each transformer block as follows: First, we use a unified self-attention layer to concurrently process both visual and text sequences. Secondly, considering the disparities between visual and text modalities, we employ distinct multilayer perceptrons (MLPs) in the feed-forward network (FFN) and linear projectors in the attention blocks to process them separately. Notably,

as shown in Fig. 3, since ViT provides visual representations with high-level semantics aligned with text, we route ViT tokens to the text branch. Finally, since the rectified flow [51] necessitates predicting the velocity at the current timestep, the timestep embedding will modulate the visual feature maps of each block via an AdaLN layer [60].

Building upon the aforementioned design, we observe that this architecture can achieve high-quality image generation outcomes without relying on the text encoder (e.g., CLIP [65] or T5 [66]) typically required in conventional T2I models [18, 32, 42]. We attribute this to the deep fusion of the LLM’s text representations and image features at each layer. Furthermore, this design enables the model to naturally inherit the long-context capabilities of the LLM, which is critical for interleaved multi-modal generation over extended sequences.

Interleaved Rotary Position Embedding Both the input and output of **Mogao** are multi-modal, so the model needs to capture three-dimensional positional relationships: H and W are used to represent the spatial positional information of the image, and T is used for the temporal positional relationship between all images and text tokens. Rotary Positional Embedding (RoPE) [70] is a widely used and effective scheme. We improved on it and proposed Interleaved RoPE (**IL-RoPE**). Different from many recent works on 3D-RoPE [1, 4, 83], we have improved the frequency allocation of each dimension and the setting of position ID for the scenario of simultaneously generating text and images.

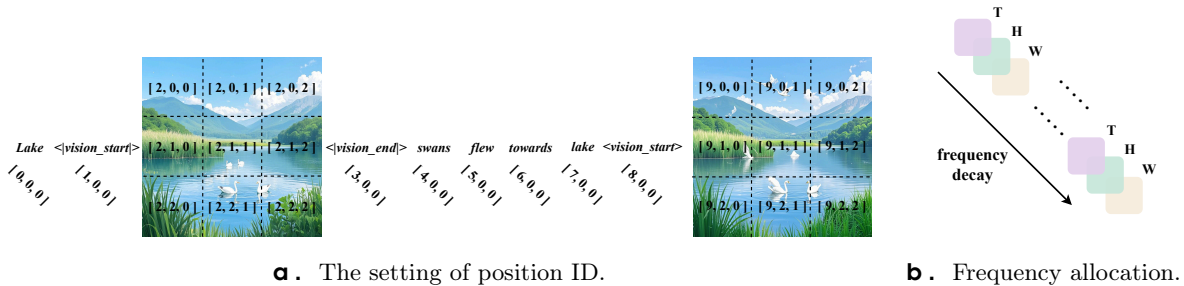


Figure 4 Interleaved 3d-RoPE.

As shown in Fig. 4a, in terms of the design of position ID, for images, the spatial position ID of H/W of each image is calculated from 0, so that all images are guaranteed to have consistent position information in space, which is conducive to image editing, multi-image generation, etc., because these tasks need to refer to previous images for generation. Meanwhile, the temporal position ID will increase for each token. Note that the temporal position ID of all tokens in an image is consistent.

In terms of frequency allocation, M-RoPE [81] proposes assigning higher frequencies to T , intermediate and lower frequencies to H and W respectively within the $d = 128$ dimensions:

$$\Theta_T = \left\{ \beta^{-\frac{2i}{d}} \mid i \in [0, 16) \right\}; \Theta_H = \left\{ \beta^{-\frac{2i}{d}} \mid i \in [16, 40) \right\}; \Theta_W = \left\{ \beta^{-\frac{2i}{d}} \mid i \in [40, 64) \right\} \quad (8)$$

where Θ denotes the rotation frequency applied to a specific dimension, and β denotes the base frequency. Such design results in the temporal dimension T focusing on capturing local relationships, while the spatial dimensions H and W prioritize long-range dependencies. This significantly degrades image generation performance, as image synthesis heavily relies on local semantic information; for instance, a 256-resolution image comprises only 16 tokens along H and W dimensions respectively [32]. Inspired by the above observation, IL-RoPE interleaves frequency assignment for $\{T, H, W\}$ within the d dimension to ensure that each dimension can capture long-range and local semantic information in a balanced manner, as demonstrated in Fig. 4b.

$$\Theta_T = \left\{ \beta^{-\frac{2i}{d}} \mid i = 3j \right\}, \Theta_H = \left\{ \beta^{-\frac{2i}{d}} \mid i = 3j + 1 \right\}, \Theta_W = \left\{ \beta^{-\frac{2i}{d}} \mid i = 3j + 2 \right\} \quad (9)$$

As shown in Eq. (9), we assign the first 48 channels to $T/H/W$ dimension alternately, and then assign the left 16 channels to T dimension for modeling long sequences.

Multi-modal Classifier-free Guidance Following previous works, we use Classifier-free guidance (CFG) [27] to enhance generation quality, which combines conditional predictions with unconditional predictions to yield results that more closely align with the specified conditions:

$$\nabla_{\mathbf{x}} \log p(\mathbf{x} | \mathbf{c}) = \gamma (\nabla_{\mathbf{x}} \log p(\mathbf{x} | \mathbf{c}) - \nabla_{\mathbf{x}} \log p(\mathbf{x})) + \nabla_{\mathbf{x}} \log p(\mathbf{x}) \quad (10)$$

where \mathbf{c} and γ denote the condition and CFG coefficient respectively. The condition of T2I models consists only of the text modality \mathbf{c}_{txt} , but in the interleaved multi-modal generation scenario presented in this paper, condition \mathbf{c} can be decomposed into two modalities \mathbf{c}_{txt} and \mathbf{c}_{img} . In practice, we observe that the image within the condition serves as a shortcut for the model in generating the subsequent image, resulting in a phenomenon akin to temporal stagnation [47]. Inspired by [6], we introduce distinct CFG coefficients γ and γ_{img} to control the influence of different modalities:

$$\begin{aligned} \nabla_{\mathbf{x}} \log p(\mathbf{x} | \mathbf{c}_{\text{img}}, \mathbf{c}_{\text{txt}}) &= \gamma (\nabla_{\mathbf{x}} \log p(\mathbf{x} | \mathbf{c}_{\text{img}}, \mathbf{c}_{\text{txt}}) - \nabla_{\mathbf{x}} \log p(\mathbf{x} | \mathbf{c}_{\text{img}})) + \\ &\quad \gamma_{\text{img}} (\nabla_{\mathbf{x}} \log p(\mathbf{x} | \mathbf{c}_{\text{img}}) - \nabla_{\mathbf{x}} \log p(\mathbf{x})) + \nabla_{\mathbf{x}} \log p(\mathbf{x}) \end{aligned} \quad (11)$$

Note that when $\gamma_{\text{img}} = \gamma$, Eq. (11) degrades to Eq. (10), where the frequently used cross-modal CFG coefficient may be too large for the intra-modal condition. This enables us to effectively regulate the influence of different modalities on image generation. We use the CFG coefficient $\gamma = 7.5$ and $\gamma_{\text{img}} = 1.5$ respectively.

3.2 Data

We use a mixture of text-only, visual understanding, image generation, and interleaved multi-modal data to train our model. The text-only and visual understanding data are inherited from DouBao LM and VLM datasets. We leverage the image generation data used to train SeedDream [25] for improving image quality and diversity. As for multimodal interleaved data, we curate it from publicly available websites and videos. For data with native texts and images, we keep the original item order during training. For video clips, we train a vision-language model to get the caption of each frame sampled from the clip. The training sample is composed of sampled frames and captions in an intertwined manner.

3.3 Training

Native Resolution The strategy of resizing images to a fixed resolution is evidently suboptimal, as it simultaneously reduces the efficiency of model training and inference while substantially limiting the model’s visual understanding capabilities [15, 34, 81]. Consequently, throughout the entire training phase, we adopt a native resolution strategy, converting input images into a variable number of visual tokens while preserving their aspect ratios. Furthermore, to bridge image representations between visual generation and understanding, we utilize this strategy consistently across both tasks.

Global Batch Reduced Loss When training with mixed-source multi-modal data on multiple GPUs, we need to carefully balance losses of tokens with variable weights to achieve a good trade-off among tasks. Suppose on n -th GPU, the i -th token has loss \mathcal{L}_i^n with weight w_i^n , it is ideal to take tokens on all GPUs as a global batch and compute the gradient with respect to model parameter W by $\frac{\partial}{\partial W} \left(\frac{\sum_n \sum_i w_i^n \mathcal{L}_i^n}{\sum_n \sum_i w_i^n} \right)$. However, it requires gathering the weights and losses of tokens on all ranks, which will definitely harm training efficiency due to the large amount of communication cost. An approximate method used frequently is to compute per-rank loss and average gradient among GPUs, i.e., $\frac{1}{N} \sum_n \frac{\partial}{\partial W} \left(\frac{\sum_i w_i^n \mathcal{L}_i^n}{\sum_i w_i^n} \right)$. However, the gradient computed by this strategy can be biased from the ideal one. We propose to use $\frac{1}{N} \sum_n \frac{\partial}{\partial W} \left(\frac{\sum_i w_i^n \mathcal{L}_i^n}{\frac{1}{N} \sum_n \sum_i w_i^n} \right)$ as a proxy, which can be easily derived to be equal to the unbiased gradient. Specifically, we first average-reduce the sum of weights on each rank and use the reduced weight as the normalization term. The communication cost of N scalars is negligible and will not introduce any training inefficiency since we apply async-reduce in practice.

Efficient Complete Teacher Forcing In interleaved multi-modal generation where interleaved samples consist of visual and textual modalities, a critical challenge arises from the discrepancy between training and inference since all visual elements are designated to be predicted during training. Specifically, while images undergo diffusion forward processes with multi-level Gaussian noise perturbations, subsequent modalities (text or images) are trained under these noisy conditions. This introduces a domain shift between the perturbed training phase and the clean inference phase.

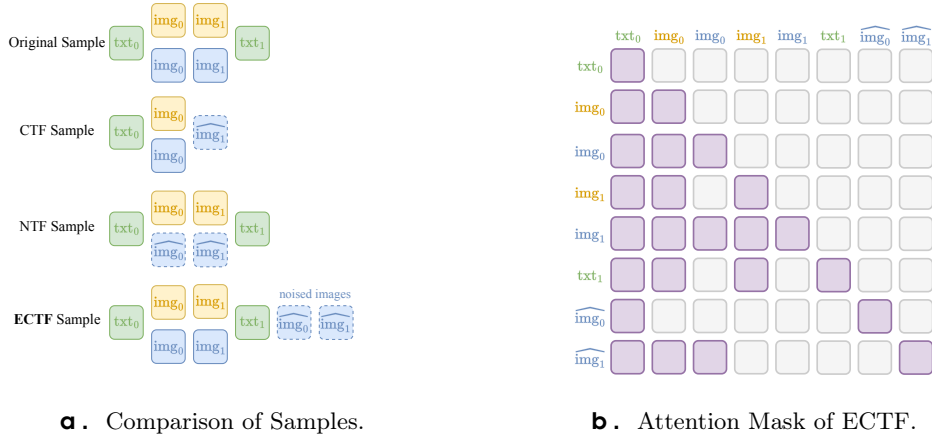


Figure 5 Efficient Complete Teacher Forcing. The VAE and ViT visual representations of an image are highlighted in blue and yellow respectively. $\widehat{\text{img}}$ indicates the noisy image. **a)** As depicted in 3.1, VAE and ViT token will share the same position id. **b)** VAE tokens can attend to all tokens, but text tokens and ViT tokens can not attend VAE tokens.

While Transfusion [96] mitigates the training-inference discrepancy via constrained noise scales, it fundamentally preserves the mismatch between iterative denoising (training) and single-pass generation (inference). Alternative methods restrict loss computation to only the final image. Despite the theoretical applicability, they suffer from compute complexity which scales quadratically with the sequence length due to duplicated computation of ahead items, making them computationally prohibitive for long multi-modal sequences.

We propose Efficient Complete Teacher Forcing (ECTF) that achieves an optimal trade-off between computational efficiency and conditional consistency. As illustrated in Fig. 5a, ECTF introduces clean-noise decoupling: clean images with interleaved sentences are separated from those noisy images through a dynamic causal attention mask in Fig. 5b, eliminating redundant computation in the last perturbation methods.

Concurrent work [97] introduces a comparable technique to our ECTF framework. However, our approach demonstrates broader versatility by effectively handling interleaved multi-modal inputs, whereas their method remains confined to visual modality processing.

4 Experiments

4.1 Experimental Setup

Implementation Details We use Qwen2.5-3B as the backbone and modify each transformer block as described in Sec. 3.1 to adapt to unified training. After transforming it into a deep-fusion architecture, the number of model parameters will double; in addition, the AdaLN-Zero layer will be added to each transformer block. Therefore, the final trainable parameter size of Mogao is 7B. It is worth noting that the deep-fusion architecture can be considered as a **fixed-routing MoE**, so its per-token computation is only **equivalent to a 3.5B model**. We use VAE from Flux [32] and ViT from Qwen2-VL [81] as the visual encoder, and the parameters of visual encoders are frozen during the entire training. During training, benefitting from the native resolution strategy, all images in all tasks do not require additional padding. Multiple samples within a batch will be packed into a sequence to enhance training efficiency.

Training Schemes The training is divided into three stages, as detailed below:

1. **Stage 1: Low-resolution unified training.** In the first stage, we conducted unified training using both multi-modal understanding data and text-to-image data. The maximum image resolution is limited to 256×256 to reduce the training difficulty on the image generation. Since we employed a pre-trained LLM that inherently possesses text generation capabilities, and we required more data to model image distributions for image generation, we adjusted the ratio of text-to-image data to multi-modal understanding data to 4:1. Meanwhile, except the visual encoder, all parameters are trainable.
2. **Stage 2: High-resolution unified training.** In this stage, we still use multi-modal understanding data and text-to-image data for training, and keep the data ratio unchanged. At the same time, we adjust the resolution from 256×256 to 512×512 to achieve higher quality generation.
3. **Stage 3: Multi-modal interleaved training.** After the previous two stages, the model has already demonstrated strong capabilities in multi-modal understanding and text-to-image generation. In the final stage, we incorporate multi-modal interleaved generated data for training. At the same time, we still include some multi-modal understanding and text-to-image datasets to maintain the model’s performance in multi-modal understanding and image generation, accounting for 20% and 40% respectively. The image resolution is maintained at 512×512 and ECTF is used to improve training efficiency.

Evaluation Setup First, we rigorously evaluate Mogao’s capabilities in image generation and multi-modal understanding through a series of comprehensive benchmarks. Then, we evaluate Mogao’s superior interleaved multi-modal generation capabilities through comprehensive and diverse qualitative results.

For multi-modal understanding, the general visual capabilities are evaluated on POPE [40], MME [19], MMBench [52], SEEDBench [36], GQA [30], and the knowledge VQA capabilities are evaluated on MMMU [94].

For the text-to-image generation, the evaluation is conducted mainly on three popular public benchmarks, i.e., GenEval [24], DPG-Bench [29], and GenAI-Bench [46]. GenEval is a challenge benchmark designed for image-to-text generation. It uses an end-to-end detector [11, 13] to evaluate the prompt-generation alignments according to the object categories, numbers, color, position, etc. It contains 553 short prompts, and we generate 4 images for every prompt for evaluation. DPG-Bench contains 1065 dense prompts and evaluates the generated images via a vision-language model [37]. GenAI-Bench contains 871 basic prompts and 1593 advanced prompts, designed for evaluation on counting, comparing, logic, etc. The performance is quantified by the VQA (visual-question-answer) score [53]. We report our evaluated results on advanced prompts.

For interleaved multi-modal generation, we first demonstrate Mogao’s zero-shot image editing capability, and then we demonstrate its automatic image and text interleaved generation, group image generation, and next frame prediction capabilities after SFT.

4.2 Interleaved Multi-Modal Generation

Visualization Fig. 2 demonstrates Mogao’s interleaved multi-modal generation capability, from which we can observe that Mogao exhibits strong ID preservation and instruction-following abilities in the interleaved generation of image and text. We highlight that high-quality and coherent text generation enables Mogao to produce accurate images based on contextual information.

Zero-Shot Image Editing Although Mogao was trained only on large-scale image-text pair data and interleaved multi-modal data without task-specific training data tailored for image editing, it demonstrates significant potential in zero-shot image editing. As illustrated in Fig. 6, Mogao can follow instructions and complete tasks such as adding, removing, and modifying elements. It can also respond well to some difficult editing instructions, such as action guidance and perspective and layout modification. Mogao is currently a pre-trained model without fine-tuning on task-specific data; we emphasize its robust generalization capabilities and the substantial potential revealed through training on interleaved multi-modal data.

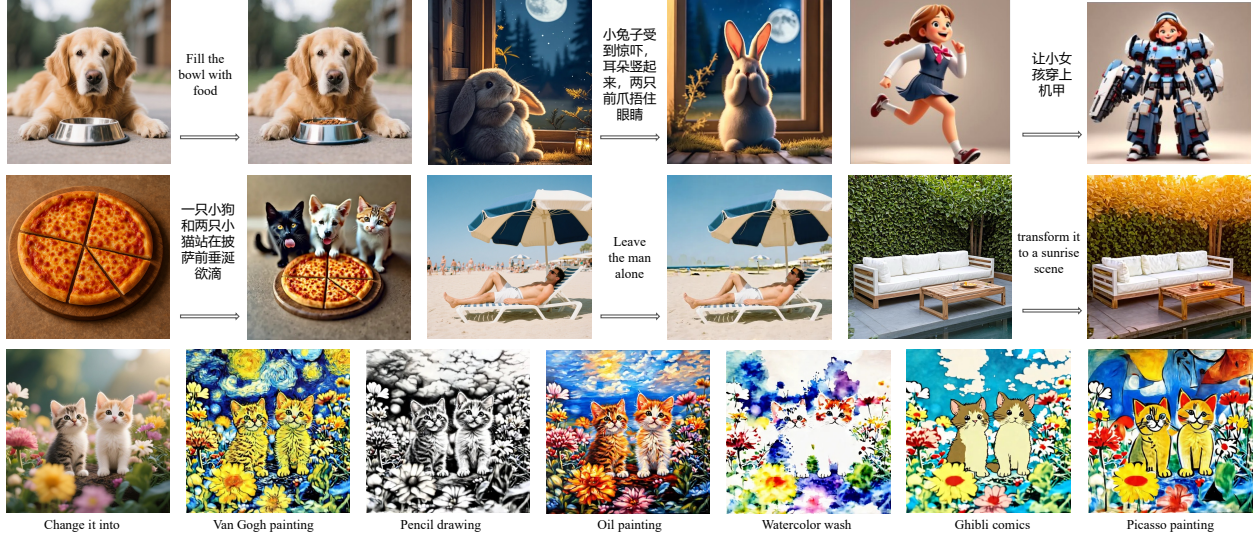


Figure 6 Mogao Zero-Shot Image Editing Visualization. The left is the original image for each group.

Table 1 Evaluation of text-to-image generation ability on GenEval benchmark.

Method	Single Obj.	Two Obj.	Counting	Colors	Position	Color Attri.	Overall \uparrow
<i>Multi-Modal Generation Models</i>							
LlamaGen [71]	0.71	0.34	0.21	0.58	0.07	0.04	0.32
LDM [69]	0.92	0.29	0.23	0.70	0.02	0.05	0.37
SDv1.5 [69]	0.97	0.38	0.35	0.76	0.04	0.06	0.43
PixArt- α [9]	0.98	0.50	0.44	0.80	0.08	0.07	0.48
SDv2.1 [69]	0.98	0.51	0.44	0.85	0.07	0.17	0.50
DALL-E 2 [67]	0.94	0.66	0.49	0.77	0.10	0.19	0.52
Emu3-Gen [82]	0.98	0.71	0.34	0.81	0.17	0.21	0.54
SDXL [61]	0.98	0.74	0.39	0.85	0.15	0.23	0.55
DALL-E 3 [5]	0.96	0.87	0.47	0.83	0.43	0.45	0.67
SD3-Medium [18]	0.99	0.94	0.72	0.89	0.33	0.60	0.74
<i>Multi-Modal Unified Models</i>							
SEED-X † [23]	0.97	0.58	0.26	0.80	0.19	0.14	0.49
Show-o [88]	0.95	0.52	0.49	0.82	0.11	0.28	0.53
D-DiT [43]	0.97	0.80	0.54	0.76	0.32	0.50	0.65
LWM [48]	0.93	0.41	0.46	0.79	0.09	0.15	0.47
Transfusion [96]	-	-	-	-	-	-	0.63
ILLUME [79]	0.99	0.86	0.45	0.71	0.39	0.28	0.61
TokenFlow-XL [62]	0.95	0.60	0.41	0.81	0.16	0.24	0.55
Chameleon [74]	-	-	-	-	-	-	0.39
Janus [84]	0.97	0.68	0.30	0.84	0.46	0.42	0.61
D-DiT [43]	0.97	0.80	0.54	0.76	0.32	0.50	0.65
Janus-Pro-1B [12]	0.98	0.82	0.51	0.89	0.65	0.56	0.73
Janus-Pro-7B [12]	0.99	0.89	0.59	0.90	0.79	0.66	0.80
Mogao-7B	1.00	0.97	0.83	0.93	0.84	0.80	0.89

4.3 Text-to-Image Generation

Benchmark Evaluation The evaluation results on GenEval [24] are shown in Table 1. Similar to previous works [12, 16, 82], we rewrite the prompts of GenEval to the format of prompts in our training set for a more comprehensive evaluation. As one can see, **Mogao** achieves comparable performance with the previous state-of-the-art unified model, i.e., Janus-Pro-7B [12]. We need to note that although **Mogao** has 7B parameters in total, the activated parameters for each token are only 3B, indicating a lower inference cost than Janus-Pro-7B. Compared to the strong generation-only model, SD3-Medium [18], **Mogao** also achieves better overall performance, especially on the scores of position. Results on DPG-Bench [29] and GenAI-Bench [46] are

Table 2 Performances on DPG-Bench.

Method	Global	Entity	Attribute	Relation	Other	Overall↑
<i>Multi-Modal Generation Models</i>						
SDv1.5 [69]	74.63	74.23	75.39	73.49	67.81	63.18
PixArt- α [9]	74.97	79.32	78.60	82.57	76.96	71.11
Lumina-Next [99]	82.82	88.65	86.44	80.53	81.82	74.63
SDXL [61]	83.27	82.43	80.91	86.76	80.41	74.65
Playground v2.5 [38]	83.06	82.59	81.20	84.08	83.50	75.47
Hunyuan-DiT [41]	84.59	80.59	88.01	74.36	86.41	78.87
PixArt- Σ [10]	86.89	82.89	88.94	86.59	87.68	80.54
Emu3-Gen [82]	85.21	86.68	86.84	90.22	83.15	80.60
DALL-E 3 [5]	90.97	89.61	88.39	90.58	89.83	83.50
SD3-Medium [18]	87.90	91.01	88.83	80.70	88.68	84.08
<i>Multi-Modal Unified Models</i>						
Janus [84]	82.33	87.38	87.70	85.46	86.41	79.68
Janus-Pro-1B [12]	87.58	88.63	88.17	88.98	88.30	82.63
Janus-Pro-7B [12]	86.90	88.90	89.40	89.32	89.48	84.19
Mogao-7B	82.37	90.03	88.26	93.18	85.40	84.33

Table 3 Comparisons on GenAI-Bench. The results are reported on the advanced prompts of GenAI-Bench.

Methods	Count↑	Differ↑	Compare↑	Logical↑		Overall↑
				Negate	Universal	
<i>Multi-Modal Generation Models</i>						
SDv2.1 [69]	0.68	0.70	0.68	0.54	0.64	0.62
SD-XL [61]	0.71	0.73	0.69	0.50	0.66	0.63
Mid-journey v6 [57]	0.78	0.78	0.79	0.50	0.76	0.69
DALL-E 3 [5]	0.82	0.78	0.82	0.48	0.80	0.70
<i>Multi-Modal Unified Models</i>						
show-o [88]	0.70	0.62	0.71	0.51	0.65	0.60
LWM [48]	0.59	0.58	0.54	0.49	0.52	0.53
VILA-U [86]	0.70	0.71	0.74	0.53	0.66	0.64
Liquid [85]	0.76	0.73	0.74	0.46	0.74	0.65
UniTok [55]	0.76	0.76	0.79	0.46	0.73	0.67
Mogao-7B	0.77	0.74	0.77	0.53	0.71	0.68

shown in Table 2 and Table 3, respectively. The conclusions on different benchmarks are consistent, showing the strong generation ability of **Mogao**.

Human Evaluation In order to better evaluate the model from the subjective perspective of humans, we have further conducted manual evaluations of Mogao and other models on the Bench-240 proposed by Seedream 2.0 [25]. The evaluations are mainly carried out from two aspects: text-image alignment, and structural correction. The evaluations are conducted by expert reviewers, and the specific evaluation strategy is consistent with that in Seedream 2.0. Expert reviewers will rate each model on a scale from 1 (indicating extreme dissatisfaction) to 5 (indicating extreme satisfaction), and the final score of a model is the arithmetic mean of the scores given by multiple reviewers.

The results in Fig. 7 demonstrate that Mogao not only performs well on open-source benchmarks but also ranks first in human evaluations across three dimensions, significantly outperforming advanced unified models such as Emu3-Gen and Janus-Pro. This suggests that Mogao has the potential to serve as a foundational model that is more practical in real-world scenarios.

Text-to-Image Visualization Mogao demonstrates remarkable aesthetic performance in image generation, as illustrated in Figure 1. Despite being fine-tuned with a limited dataset of high-quality 512×512 images, the model excels in image quality and aesthetic presentation. The generated images are impressive in composition, color manipulation, reality-virtual interplay, and emotional conveyance. In addition, Mogao’s inherent text

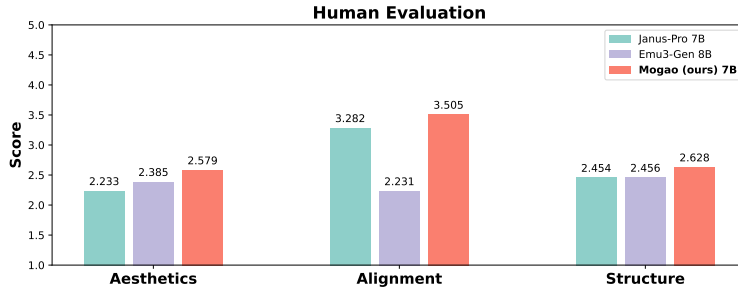


Figure 7 Human evaluation.

rendering capability allows it to generate poster-style images that push the boundaries of creativity.

4.4 Multi-modal Understanding

Table 4 Comparison with other methods on multimodal understanding benchmarks. "Avg." represents the average score over 6 benchmarks.

Model	Trainable Params	POPE	MME-P	MMB	SEED	GQA	MMMU	Avg.
<i>Multi-Modal Understanding Models</i>								
MobileVLM-V2 [14]	1.4B	84.3	1302.8	57.7	-	59.3	-	-
MobileVLM-V2 [14]	2.7B	84.7	1440.5	63.2	-	61.1	-	-
LLaVA-Phi [98]	2.7B	85.0	1335.1	59.8	-	-	-	-
LLaVA-v1.5 [50]	7B	85.9	1510.7	64.3	58.6	62.0	35.4	-
Qwen-VL-Chat [3]	7B	-	1487.5	60.6	58.2	57.5	-	-
IDEFICS [33]	8B	-	-	48.2	-	38.4	-	-
Emu3-Chat [82]	8B	85.2	1244	58.5	68.2	60.3	31.6	50.7
<i>Multi-Modal Unified Models</i>								
Show-o-512 [88]	1.3B	80.0	1097.2	-	-	58.0	26.7	-
JanusFlow [56]	1.3B	88.0	1333.1	74.9	70.5	60.3	29.3	53.9
Janus-Pro [12]	1.5B	86.2	1444.0	75.5	68.3	59.3	36.3	54.4
D-Dit [43]	2B	84.0	1124.7	-	-	59.2	-	-
ILLUME [79]	7B	88.5	1445.3	65.1	72.9	-	38.2	-
LWM [48]	7B	75.2	-	-	-	44.8	-	-
VILA-U [86]	7B	85.8	1401.8	-	59.0	60.8	-	-
Janus-Pro [12]	7B	87.4	1567.1	79.2	72.1	62.0	41.0	57.1
MMAR [90]	7B	83.0	1393.9	66.3	64.5	-	-	-
MetaMorph [76]	8B	-	-	75.2	71.8	-	-	-
TokenFlow-XL [62]	13B	86.8	1545.9	68.9	68.7	62.7	38.7	54.4
Mogao-7B (ours)	7B	88.9	1592	75.0	74.6	60.9	44.2	57.4

To evaluate Mogao’s performance on multi-modal understanding, we show a comprehensive comparison of Mogao with other methods on various public benchmarks in Tab. 4. The compared models can be divided into two categories: multi-modal understanding models and multi-modal unified models. Mogao achieved SOTA on 4 benchmarks, including POPE, MME-P, SEED, and MMMU, and obtained the highest average score over 6 benchmarks. This result shows that Mogao has well integrated the two tasks of image understanding and image generation into one model and achieved satisfying performance.

4.5 Ablation Studies

The qualitative and quantitative analysis in Sec. 4 demonstrates that Mogao is an omni-foundation model with interleaved multi-modal generation capabilities. In this section, we conducted comprehensive ablation experiments to verify the effectiveness and necessity of the key designs in Sec. 3. All ablation experiments will be conducted in a development setting. Concretely, the maximum image resolution is set to 256×256 , the 1.5B model of Qwen2 is used as the backbone, and all models are trained for 35,000 steps. The settings of different experiments and the multi-modal understanding metrics are shown in Tab. 5, and the loss curves of image generation are shown in Fig. 8.

Table 5 Ablation studies on multi-modal understanding benchmark. Experiment with underline denote the baseline settings and Mogao setting is highlighted in `gray`.

Exp. ID	Deep-Fusion	Position Embedding	Visual Encoder		Evaluation Benchmarks						
			Gen.	Und.	POPE	MME-P	MMB	SEED	GQA	MMMU	Avg.
<u>A</u>	×	M-RoPE [4]	VAE	VAE	67.2	885.9	29.9	48.2	46.7	32.8	37.5
B	×	IL-RoPE	VAE	VAE	76.4	880.3	29.2	51.8	47.2	33.3	39.7
C	×	IL-RoPE	VAE	VAE + ViT	86.6	1302.6	62.5	68.4	56.9	35.3	51.7
D (Mogao)	✓	IL-RoPE	VAE	VAE + ViT	87.3	1353.6	65.9	66.8	58.3	36.7	52.6

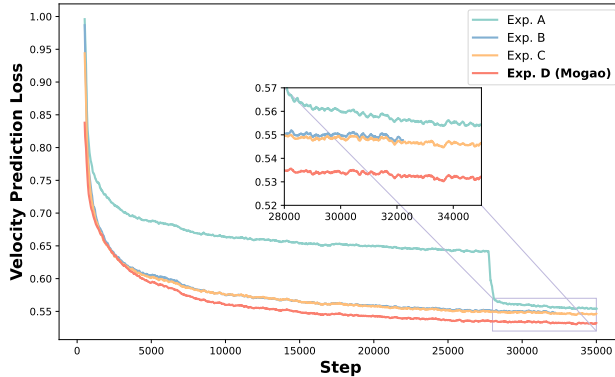


Figure 8 Ablation studies on flow matching loss. According to our experimental experience, a reduction in the velocity prediction loss of **0.001-level** will lead to a significant improvement in image generation.

Position Embedding for Unified Model As shown in Fig. 8, the comparison between Exp. A and Exp. B demonstrates that the IL-RoPE proposed in this paper has a significant advantage in image generation, and its loss converges faster and is lower. We attribute this to the reasonable frequency allocation detailed in Sec. 3.1. In contrast, the unreasonable frequency allocation strategy of M-RoPE in the H and W dimensions leads to a slower loss convergence speed.

Enhance Multi-Modal Understanding with Dual Visual Encoder Comparing Exp. B and Exp. C in Tab. 5, we can find that the image representation with high-level semantics from ViT significantly enhances Mogao’s multi-modal understanding ability. Furthermore, we can observe that Exp. C has a lower image generation loss in Fig. 8. This is because diffusion focuses more on modeling low-frequency semantics and image structure in the high-noise stage, while the additional visual representation from ViT added during training can help the model better learn high-level semantics. Similar findings can be found in REPA [93].

Deep-Fusion Architecture In Exp. C, the image and text modalities share parameters in the backbone, while Exp. D adopts the deep fusion architecture described in Sec. 3.1. As depicted in Fig. 8 and Tab. 5, the flow matching loss of Exp. D is significantly reduced compared to Exp. C, and the average score over 6 multi-modal understanding benchmarks is further improved. We attribute this phenomenon to the fact that multi-modal understanding tasks favor low-frequency, high-level semantic representations, while generation tasks, particularly in the low-noise stage, prioritize high-frequency, low-level detail representations [68]. Thus, decoupling understanding and generation within the backbone enhances the performance of both tasks effectively.

5 Conclusion

We introduce Mogao, an omni-foundation model for interleaved multi-modal generation. We first propose several key model architecture designs to seamlessly integrate autoregressive and diffusion models in Mogao, which enable Mogao to achieve excellent multi-modal understanding and image generation capabilities. Based

on the strong single-modal generation capabilities, Mogao unlocks more powerful interleaved multi-modal generation capabilities than previous unified models by performing causal interleaved generation at the modal level. Through an efficient large-scale training process utilizing interleaved multi-modal data, Mogao not only excels in multi-modal generation tasks but also exhibits competitive emergent capabilities, such as zero-shot image editing and element composition, with strong consistency. Overall, unified models demonstrate greater potential compared to single-modal generation approaches. We hope that Mogao will inspire further exploration to advance the development of general artificial intelligence.

References

- [1] Pravesh Agrawal, Szymon Antoniak, Emma Bou Hanna, Baptiste Bout, Devendra Chaplot, Jessica Chudnovsky, Diogo Costa, Baudouin De Monicault, Saurabh Garg, Theophile Gervet, et al. Pixtral 12b. [arXiv preprint arXiv:2410.07073](#), 2024.
- [2] Jean-Baptiste Alayrac, Jeff Donahue, Pauline Luc, Antoine Miech, Iain Barr, Yana Hasson, Karel Lenc, Arthur Mensch, Katherine Millican, Malcolm Reynolds, et al. Flamingo: a visual language model for few-shot learning. *Advances in neural information processing systems*, 35:23716–23736, 2022.
- [3] Jinze Bai, Shuai Bai, Shusheng Yang, Shijie Wang, Sinan Tan, Peng Wang, Junyang Lin, Chang Zhou, and Jingren Zhou. Qwen-vl: A frontier large vision-language model with versatile abilities. [arXiv preprint arXiv:2308.12966](#), 2023.
- [4] Shuai Bai, Keqin Chen, Xuejing Liu, Jialin Wang, Wenbin Ge, Sibong Song, Kai Dang, Peng Wang, Shijie Wang, Jun Tang, et al. Qwen2. 5-vl technical report. [arXiv preprint arXiv:2502.13923](#), 2025.
- [5] James Betker, Gabriel Goh, Li Jing, Tim Brooks, Jianfeng Wang, Linjie Li, Long Ouyang, Juntang Zhuang, Joyce Lee, Yufei Guo, et al. Improving image generation with better captions. *Computer Science*. <https://cdn.openai.com/papers/dall-e-3.pdf>, 2(3):8, 2023.
- [6] Tim Brooks, Aleksander Holynski, and Alexei A Efros. Instructpix2pix: Learning to follow image editing instructions. In *Proceedings of the IEEE/CVF Conference on Computer Vision and Pattern Recognition*, pages 18392–18402, 2023.
- [7] Tom B. Brown, Benjamin Mann, Nick Ryder, Melanie Subbiah, Jared Kaplan, Prafulla Dhariwal, et al. Language models are few-shot learners. *Advances in Neural Information Processing Systems*, 33:1877–1901, 2020.
- [8] Huiwen Chang, Han Zhang, Lu Jiang, Ce Liu, and William T Freeman. Maskgit: Masked generative image transformer. In *Proceedings of the IEEE/CVF conference on computer vision and pattern recognition*, pages 11315–11325, 2022.
- [9] Junsong Chen, Jincheng Yu, Chongjian Ge, Lewei Yao, Enze Xie, Yue Wu, Zhongdao Wang, James Kwok, Ping Luo, Huchuan Lu, et al. Pixart-*alpha*: Fast training of diffusion transformer for photorealistic text-to-image synthesis. [arXiv preprint arXiv:2310.00426](#), 2023.
- [10] Junsong Chen, Chongjian Ge, Enze Xie, Yue Wu, Lewei Yao, Xiaozhe Ren, Zhongdao Wang, Ping Luo, Huchuan Lu, and Zhenguo Li. PixArt-Sigma: Weak-to-strong training of diffusion transformer for 4K text-to-image generation. [arXiv preprint arXiv:2403.04692](#), 2024.
- [11] Kai Chen, Jiaqi Wang, Jiangmiao Pang, Yuhang Cao, Yu Xiong, Xiaoxiao Li, Shuyang Sun, Wansen Feng, Ziwei Liu, Jiarui Xu, Zheng Zhang, Dazhi Cheng, Chenchen Zhu, Tianheng Cheng, Qijie Zhao, Buyu Li, Xin Lu, Rui Zhu, Yue Wu, Jifeng Dai, Jingdong Wang, Jianping Shi, Wanli Ouyang, Chen Change Loy, and Dahua Lin. Mmdetection: Open mmlab detection toolbox and benchmark, 2019. URL <https://arxiv.org/abs/1906.07155>.
- [12] Xiaokang Chen, Zhiyu Wu, Xingchao Liu, Zizheng Pan, Wen Liu, Zhenda Xie, Xingkai Yu, and Chong Ruan. Janus-pro: Unified multimodal understanding and generation with data and model scaling. [arXiv preprint arXiv:2501.17811](#), 2025.
- [13] Bowen Cheng, Ishan Misra, Alexander G. Schwing, Alexander Kirillov, and Rohit Girdhar. Masked-attention mask transformer for universal image segmentation, 2022. URL <https://arxiv.org/abs/2112.01527>.
- [14] Xiangxiang Chu, Limeng Qiao, Xinyu Zhang, Shuang Xu, Fei Wei, Yang Yang, Xiaofei Sun, Yiming Hu, Xinyang Lin, Bo Zhang, et al. Mobilevlm v2: Faster and stronger baseline for vision language model. [arXiv preprint arXiv:2402.03766](#), 2024.
- [15] Mostafa Dehghani, Basil Mustafa, Josip Djolonga, Jonathan Heek, Matthias Minderer, Mathilde Caron, Andreas Steiner, Joan Puigcerver, Robert Geirhos, Ibrahim M Alabdulmohsin, et al. Patch n’pack: Navit, a vision transformer for any aspect ratio and resolution. *Advances in Neural Information Processing Systems*, 36:2252–2274, 2023.
- [16] Haoge Deng, Ting Pan, Haiwen Diao, Zhengxiong Luo, Yufeng Cui, Huchuan Lu, Shiguang Shan, Yonggang Qi, and Xinlong Wang. Autoregressive video generation without vector quantization. [arXiv preprint arXiv:2412.14169](#), 2024.

- [17] Patrick Esser, Robin Rombach, and Bjorn Ommer. Taming transformers for high-resolution image synthesis. In *Proceedings of the IEEE/CVF conference on computer vision and pattern recognition*, pages 12873–12883, 2021.
- [18] Patrick Esser, Sumith Kulal, Andreas Blattmann, Rahim Entezari, Jonas Müller, Harry Saini, Yam Levi, Dominik Lorenz, Axel Sauer, Frederic Boesel, et al. Scaling rectified flow transformers for high-resolution image synthesis. In *Forty-first International Conference on Machine Learning*, 2024.
- [19] Chaoyou Fu, Peixian Chen, Yunhang Shen, Yulei Qin, Mengdan Zhang, Xu Lin, Jinrui Yang, Xiawu Zheng, Ke Li, Xing Sun, et al. Mme: A comprehensive evaluation benchmark for multimodal large language models. *arXiv preprint arXiv:2306.13394*, 2023.
- [20] Yu Gao, Lixue Gong, Qiushan Guo, Xiaoxia Hou, Zhichao Lai, Fanshi Li, Liang Li, Xiaochen Lian, Chao Liao, Liyang Liu, et al. Seedream 3.0 technical report. *arXiv preprint arXiv:2504.11346*, 2025.
- [21] Yuying Ge, Yixiao Ge, Ziyun Zeng, Xintao Wang, and Ying Shan. Planting a seed of vision in large language model. *arXiv preprint arXiv:2307.08041*, 2023.
- [22] Yuying Ge, Sijie Zhao, Ziyun Zeng, Yixiao Ge, Chen Li, Xintao Wang, and Ying Shan. Making llama see and draw with seed tokenizer. *arXiv preprint arXiv:2310.01218*, 2023.
- [23] Yuying Ge, Sijie Zhao, Jinguo Zhu, Yixiao Ge, Kun Yi, Lin Song, Chen Li, Xiaohan Ding, and Ying Shan. Seed-x: Multimodal models with unified multi-granularity comprehension and generation. *arXiv preprint arXiv:2404.14396*, 2024.
- [24] Dhruva Ghosh, Hannaneh Hajishirzi, and Ludwig Schmidt. Geneval: An object-focused framework for evaluating text-to-image alignment. *Advances in Neural Information Processing Systems*, 36:52132–52152, 2023.
- [25] Lixue Gong, Xiaoxia Hou, Fanshi Li, Liang Li, Xiaochen Lian, Fei Liu, Liyang Liu, Wei Liu, Wei Lu, Yichun Shi, Shiqi Sun, Yu Tian, Zhi Tian, Peng Wang, Xun Wang, Ye Wang, Guofeng Wu, Jie Wu, Xin Xia, Xuefeng Xiao, Linjie Yang, Zhonghua Zhai, Xinyu Zhang, Qi Zhang, Yuwei Zhang, Shijia Zhao, Jianchao Yang, and Weilin Huang. Seedream 2.0: A native chinese-english bilingual image generation foundation model, 2025. URL <https://arxiv.org/abs/2503.07703>.
- [26] Jian Han, Jinlai Liu, Yi Jiang, Bin Yan, Yuqi Zhang, Zehuan Yuan, Bingyue Peng, and Xiaobing Liu. Infinity: Scaling bitwise autoregressive modeling for high-resolution image synthesis. *arXiv preprint arXiv:2412.04431*, 2024.
- [27] Jonathan Ho and Tim Salimans. Classifier-free diffusion guidance. *arXiv preprint arXiv:2207.12598*, 2022.
- [28] Jonathan Ho, Ajay Jain, and Pieter Abbeel. Denoising diffusion probabilistic models. *Advances in neural information processing systems*, 33:6840–6851, 2020.
- [29] Xiwei Hu, Rui Wang, Yixiao Fang, Bin Fu, Pei Cheng, and Gang Yu. Ella: Equip diffusion models with llm for enhanced semantic alignment, 2024.
- [30] Drew A Hudson and Christopher D Manning. Gqa: A new dataset for real-world visual reasoning and compositional question answering. In *Proceedings of the IEEE/CVF conference on computer vision and pattern recognition*, pages 6700–6709, 2019.
- [31] Diederik P Kingma and Max Welling. Auto-encoding variational bayes. *arXiv preprint arXiv:1312.6114*, 2013.
- [32] Black Forest Labs. Flux. <https://github.com/black-forest-labs/flux>, 2023.
- [33] Hugo Laurençon, Daniel van Strien, Stas Bekman, Leo Tronchon, Lucile Saulnier, Thomas Wang, Siddharth Karamcheti, Amanpreet Singh, Giada Pistilli, Yacine Jernite, and et al. Introducing idefics: An open reproduction of state-of-the-art visual language model, 2023. URL <https://huggingface.co/blog/idefics>.
- [34] Kenton Lee, Mandar Joshi, Iulia Raluca Turc, Hexiang Hu, Fangyu Liu, Julian Martin Eisenschlos, Urvashi Khandelwal, Peter Shaw, Ming-Wei Chang, and Kristina Toutanova. Pix2struct: Screenshot parsing as pretraining for visual language understanding. In *International Conference on Machine Learning*, pages 18893–18912. PMLR, 2023.
- [35] Bo Li, Yuanhan Zhang, Dong Guo, Renrui Zhang, Feng Li, Hao Zhang, Kaichen Zhang, Peiyuan Zhang, Yanwei Li, Ziwei Liu, et al. Llava-onevision: Easy visual task transfer. *arXiv preprint arXiv:2408.03326*, 2024.
- [36] Bohao Li, Rui Wang, Guangzhi Wang, Yuying Ge, Yixiao Ge, and Ying Shan. Seed-bench: Benchmarking multimodal llms with generative comprehension. *arXiv preprint arXiv:2307.16125*, 2023.

- [37] Chenliang Li et al. mplug: Effective and efficient vision-language learning by cross-modal skip-connections. *EMNLP*, 2022.
- [38] Daiqing Li, Aleks Kamko, Ehsan Akhgari, Ali Sabet, Linmiao Xu, and Suhail Doshi. Playground v2.5: Three insights towards enhancing aesthetic quality in text-to-image generation. *arXiv preprint arXiv:2402.17245*, 2024.
- [39] Tianhong Li, Yonglong Tian, He Li, Mingyang Deng, and Kaiming He. Autoregressive image generation without vector quantization. *Advances in Neural Information Processing Systems*, 37:56424–56445, 2025.
- [40] Yifan Li, Yifan Du, Kun Zhou, Jinpeng Wang, Wayne Xin Zhao, and Ji-Rong Wen. Evaluating object hallucination in large vision-language models. *arXiv preprint arXiv:2305.10355*, 2023.
- [41] Zhimin Li, Jianwei Zhang, Qin Lin, Jiangfeng Xiong, Yanxin Long, Xincheng Deng, Yingfang Zhang, Xingchao Liu, Minbin Huang, Zedong Xiao, et al. Hunyuan-DiT: A powerful multi-resolution diffusion transformer with fine-grained chinese understanding. *arXiv preprint arXiv:2405.08748*, 2024.
- [42] Zhimin Li, Jianwei Zhang, Qin Lin, Jiangfeng Xiong, Yanxin Long, Xincheng Deng, Yingfang Zhang, Xingchao Liu, Minbin Huang, Zedong Xiao, et al. Hunyuan-dit: A powerful multi-resolution diffusion transformer with fine-grained chinese understanding. *arXiv preprint arXiv:2405.08748*, 2024.
- [43] Zijie Li, Henry Li, Yichun Shi, Amir Barati Farimani, Yuval Kluger, Linjie Yang, and Peng Wang. Dual diffusion for unified image generation and understanding. *arXiv preprint arXiv:2501.00289*, 2024.
- [44] Weixin Liang, Lili Yu, Liang Luo, Srinivasan Iyer, Ning Dong, Chunting Zhou, Gargi Ghosh, Mike Lewis, Wen-tau Yih, Luke Zettlemoyer, et al. Mixture-of-transformers: A sparse and scalable architecture for multi-modal foundation models. *arXiv preprint arXiv:2411.04996*, 2024.
- [45] Xi Victoria Lin, Akshat Shrivastava, Liang Luo, Srinivasan Iyer, Mike Lewis, Gargi Ghosh, Luke Zettlemoyer, and Armen Aghajanyan. Moma: Efficient early-fusion pre-training with mixture of modality-aware experts. *arXiv preprint arXiv:2407.21770*, 2024.
- [46] Zhiqiu Lin, Deepak Pathak, Baiqi Li, Jiayao Li, Xide Xia, Graham Neubig, Pengchuan Zhang, and Deva Ramanan. Evaluating text-to-visual generation with image-to-text generation. *arXiv preprint arXiv:2404.01291*, 2024.
- [47] Zongyu Lin, Wei Liu, Chen Chen, Jiasen Lu, Wenze Hu, Tsu-Jui Fu, Jesse Allardice, Zhengfeng Lai, Liangchen Song, Bowen Zhang, et al. Stiv: Scalable text and image conditioned video generation. *arXiv preprint arXiv:2412.07730*, 2024.
- [48] Hao Liu, Wilson Yan, Matei Zaharia, and Pieter Abbeel. World model on million-length video and language with ringattention. *arXiv e-prints*, pages arXiv–2402, 2024.
- [49] Haotian Liu, Chunyuan Li, Qingyang Wu, and Yong Jae Lee. Visual instruction tuning. *Advances in neural information processing systems*, 36:34892–34916, 2023.
- [50] Haotian Liu, Chunyuan Li, Yuheng Li, and Yong Jae Lee. Improved baselines with visual instruction tuning. In *Proceedings of the IEEE/CVF Conference on Computer Vision and Pattern Recognition*, pages 26296–26306, 2024.
- [51] Xingchao Liu, Chengyue Gong, and Qiang Liu. Flow straight and fast: Learning to generate and transfer data with rectified flow. *arXiv preprint arXiv:2209.03003*, 2022.
- [52] Yuan Liu, Haodong Duan, Yuanhan Zhang, Bo Li, Songyang Zhang, Wangbo Zhao, Yike Yuan, Jiaqi Wang, Conghui He, Ziwei Liu, et al. Mmbench: Is your multi-modal model an all-around player? *arXiv preprint arXiv:2307.06281*, 2023.
- [53] Shayne et al. Longpre. The flan collection: Designing data and methods for effective instruction tuning. *arXiv:2301.13688*, 2023.
- [54] Haoyu Lu, Wen Liu, Bo Zhang, Bingxuan Wang, Kai Dong, Bo Liu, Jingxiang Sun, Tongzheng Ren, Zhuoshu Li, Hao Yang, et al. Deepseek-vl: towards real-world vision-language understanding. *arXiv preprint arXiv:2403.05525*, 2024.
- [55] Chuofan Ma, Yi Jiang, Junfeng Wu, Jihan Yang, Xin Yu, Zehuan Yuan, Bingyue Peng, and Xiaojuan Qi. Unitok: A unified tokenizer for visual generation and understanding. *arXiv preprint arXiv:2502.20321*, 2025.

- [56] Yiyang Ma, Xingchao Liu, Xiaokang Chen, Wen Liu, Chengyue Wu, Zhiyu Wu, Zizheng Pan, Zhenda Xie, Haowei Zhang, Liang Zhao, et al. Janusflow: Harmonizing autoregression and rectified flow for unified multimodal understanding and generation. arXiv preprint arXiv:2411.07975, 2024.
- [57] Midjourney. Midjourney v6.1. <https://www.midjourney.com/>, 2024.
- [58] OpenAI, :, Aaron Hurst, and Adam Lerer et al. Gpt-4o system card, 2024. URL <https://arxiv.org/abs/2410.21276>.
- [59] Maxime Oquab, Timothée Darcet, Théo Moutakanni, Huy Vo, Marc Szafraniec, Vasil Khalidov, Pierre Fernandez, Daniel Haziza, Francisco Massa, Alaaeldin El-Nouby, et al. Dinov2: Learning robust visual features without supervision. arXiv preprint arXiv:2304.07193, 2023.
- [60] William Peebles and Saining Xie. Scalable diffusion models with transformers. In Proceedings of the IEEE/CVF international conference on computer vision, pages 4195–4205, 2023.
- [61] Dustin Podell, Zion English, Kyle Lacey, Andreas Blattmann, Tim Dockhorn, Jonas Müller, Joe Penna, and Robin Rombach. Sd-xl: Improving latent diffusion models for high-resolution image synthesis. arXiv preprint arXiv:2307.01952, 2023.
- [62] Liao Qu, Huichao Zhang, Yiheng Liu, Xu Wang, Yi Jiang, Yiming Gao, Hu Ye, Daniel K Du, Zehuan Yuan, and Xinglong Wu. Tokenflow: Unified image tokenizer for multimodal understanding and generation. arXiv preprint arXiv:2412.03069, 2024.
- [63] Alec Radford, Karthik Narasimhan, Tim Salimans, and Ilya Sutskever. Improving language understanding by generative pre-training. 2018.
- [64] Alec Radford, Jeffrey Wu, Rewon Child, David Luan, Dario Amodei, and Ilya Sutskever. Language models are unsupervised multitask learners. 2019.
- [65] Alec Radford, Jong Wook Kim, Chris Hallacy, Aditya Ramesh, Gabriel Goh, Sandhini Agarwal, Girish Sastry, Amanda Askell, Pamela Mishkin, Jack Clark, et al. Learning transferable visual models from natural language supervision. In International conference on machine learning, pages 8748–8763. PMLR, 2021.
- [66] Colin Raffel, Noam Shazeer, Adam Roberts, Katherine Lee, Sharan Narang, Michael Matena, Yanqi Zhou, Wei Li, and Peter J Liu. Exploring the limits of transfer learning with a unified text-to-text transformer. Journal of machine learning research, 21(140):1–67, 2020.
- [67] Aditya Ramesh, Prafulla Dhariwal, Alex Nichol, Casey Chu, and Mark Chen. Hierarchical text-conditional image generation with clip latents. arXiv preprint arXiv:2204.06125, 1(2):3, 2022.
- [68] Severi Rissanen, Markus Heinonen, and Arno Solin. Generative modelling with inverse heat dissipation. arXiv preprint arXiv:2206.13397, 2022.
- [69] Robin Rombach, Andreas Blattmann, Dominik Lorenz, Patrick Esser, and Björn Ommer. High-resolution image synthesis with latent diffusion models. In Proceedings of the IEEE/CVF conference on computer vision and pattern recognition, pages 10684–10695, 2022.
- [70] Jianlin Su, Murtadha Ahmed, Yu Lu, Shengfeng Pan, Wen Bo, and Yunfeng Liu. Roformer: Enhanced transformer with rotary position embedding. Neurocomputing, 568:127063, 2024.
- [71] Peize Sun, Yi Jiang, Shoufa Chen, Shilong Zhang, Bingyue Peng, Ping Luo, and Zehuan Yuan. Autoregressive model beats diffusion: Llama for scalable image generation. arXiv preprint arXiv:2406.06525, 2024.
- [72] Quan Sun, Yufeng Cui, Xiaosong Zhang, Fan Zhang, Qiying Yu, Zhengxiong Luo, Yuezhe Wang, Yongming Rao, Jingjing Liu, Tiejun Huang, et al. Generative multimodal models are in-context learners. arXiv e-prints, pages arXiv–2312, 2023.
- [73] Quan Sun, Qiying Yu, Yufeng Cui, Fan Zhang, Xiaosong Zhang, Yuezhe Wang, Hongcheng Gao, Jingjing Liu, Tiejun Huang, and Xinlong Wang. Emu: Generative pretraining in multimodality. arXiv preprint arXiv:2307.05222, 2023.
- [74] Chameleon Team. Chameleon: Mixed-modal early-fusion foundation models. arXiv preprint arXiv:2405.09818, 2024.

- [75] Keyu Tian, Yi Jiang, Zehuan Yuan, Bingyue Peng, and Liwei Wang. Visual autoregressive modeling: Scalable image generation via next-scale prediction. *Advances in neural information processing systems*, 37:84839–84865, 2025.
- [76] Shengbang Tong, David Fan, Jiachen Zhu, Yunyang Xiong, Xinlei Chen, Koustuv Sinha, Michael Rabbat, Yann LeCun, Saining Xie, and Zhuang Liu. Metamorph: Multimodal understanding and generation via instruction tuning. *arXiv preprint arXiv:2412.14164*, 2024.
- [77] Hugo Touvron, Thibaut Lavril, Gautier Izacard, Xavier Martinet, Marie-Anne Lachaux, Timothée Lacroix, Baptiste Rozière, Naman Goyal, Eric Hambro, Faisal Azhar, et al. Llama: Open and efficient foundation language models. *arXiv preprint arXiv:2302.13971*, 2023.
- [78] Ashish Vaswani, Noam Shazeer, Niki Parmar, Jakob Uszkoreit, Llion Jones, Aidan N Gomez, Łukasz Kaiser, and Illia Polosukhin. Attention is all you need. *Advances in neural information processing systems*, 30, 2017.
- [79] Chunwei Wang, Guansong Lu, Junwei Yang, Runhui Huang, Jianhua Han, Lu Hou, Wei Zhang, and Hang Xu. Illume: Illuminating your llms to see, draw, and self-enhance. *arXiv preprint arXiv:2412.06673*, 2024.
- [80] Junke Wang, Zhi Tian, Xun Wang, Xinyu Zhang, Weilin Huang, Zuxuan Wu, and Yu-Gang Jiang. Simplear: Pushing the frontier of autoregressive visual generation through pretraining, sft, and rl. *arXiv preprint arXiv:2504.11455*, 2025.
- [81] Peng Wang, Shuai Bai, Sinan Tan, Shijie Wang, Zhihao Fan, Jinze Bai, Keqin Chen, Xuejing Liu, Jialin Wang, Wenbin Ge, et al. Qwen2-vl: Enhancing vision-language model’s perception of the world at any resolution. *arXiv preprint arXiv:2409.12191*, 2024.
- [82] Xinlong Wang, Xiaosong Zhang, Zhengxiong Luo, Quan Sun, Yufeng Cui, Jinsheng Wang, Fan Zhang, Yueze Wang, Zhen Li, Qiyong Yu, et al. Emu3: Next-token prediction is all you need. *arXiv preprint arXiv:2409.18869*, 2024.
- [83] Xilin Wei, Xiaoran Liu, Yuhang Zang, Xiaoyi Dong, Pan Zhang, Yuhang Cao, Jian Tong, Haodong Duan, Qipeng Guo, Jiaqi Wang, et al. Videorope: What makes for good video rotary position embedding? *arXiv preprint arXiv:2502.05173*, 2025.
- [84] Chengyue Wu, Xiaokang Chen, Zhiyu Wu, Yiyang Ma, Xingchao Liu, Zizheng Pan, Wen Liu, Zhenda Xie, Xingkai Yu, Chong Ruan, et al. Janus: Decoupling visual encoding for unified multimodal understanding and generation. *arXiv preprint arXiv:2410.13848*, 2024.
- [85] Junfeng Wu, Yi Jiang, Chuofan Ma, Yuliang Liu, Hengshuang Zhao, Zehuan Yuan, Song Bai, and Xiang Bai. Liquid: Language models are scalable multi-modal generators. *arXiv preprint arXiv:2412.04332*, 2024.
- [86] Yecheng Wu, Zhuoyang Zhang, Junyu Chen, Haotian Tang, Dacheng Li, Yunhao Fang, Ligeng Zhu, Enze Xie, Hongxu Yin, Li Yi, et al. Vila-u: a unified foundation model integrating visual understanding and generation. *arXiv preprint arXiv:2409.04429*, 2024.
- [87] Shitao Xiao, Yueze Wang, Junjie Zhou, Huaying Yuan, Xingrun Xing, Ruiran Yan, Shuting Wang, Tiejun Huang, and Zheng Liu. Omnigen: Unified image generation. *arXiv preprint arXiv:2409.11340*, 2024.
- [88] Jinheng Xie, Weijia Mao, Zechen Bai, David Junhao Zhang, Weihao Wang, Kevin Qinghong Lin, Yuchao Gu, Zhijie Chen, Zhenheng Yang, and Mike Zheng Shou. Show-o: One single transformer to unify multimodal understanding and generation. *arXiv preprint arXiv:2408.12528*, 2024.
- [89] An Yang, Baosong Yang, Beichen Zhang, Binyuan Hui, Bo Zheng, Bowen Yu, Chengyuan Li, Dayiheng Liu, Fei Huang, Haoran Wei, et al. Qwen2. 5 technical report. *arXiv preprint arXiv:2412.15115*, 2024.
- [90] Jian Yang, Dacheng Yin, Yizhou Zhou, Fengyun Rao, Wei Zhai, Yang Cao, and Zheng-Jun Zha. Mmar: Towards lossless multi-modal auto-regressive probabilistic modeling. *arXiv preprint arXiv:2410.10798*, 2024.
- [91] Lili Yu, Bowen Shi, Ramakanth Pasunuru, Benjamin Muller, Olga Golovneva, Tianlu Wang, Arun Babu, Binh Tang, Brian Karrer, Shelly Sheynin, Candace Ross, Adam Polyak, Russell Howes, Vasu Sharma, Puxin Xu, Hovhannes Tamoyan, Oron Ashual, Uriel Singer, Shang-Wen Li, Susan Zhang, Richard James, Gargi Ghosh, Yaniv Taigman, Maryam Fazel-Zarandi, Asli Celikyilmaz, Luke Zettlemoyer, and Armen Aghajanyan. Scaling autoregressive multi-modal models: Pretraining and instruction tuning, 2023. URL <https://arxiv.org/abs/2309.02591>.
- [92] Qihang Yu, Ju He, Xueqing Deng, Xiaohui Shen, and Liang-Chieh Chen. Randomized autoregressive visual generation. *arXiv preprint arXiv:2411.00776*, 2024.

- [93] Sihyun Yu, Sangkyung Kwak, Huiwon Jang, Jongheon Jeong, Jonathan Huang, Jinwoo Shin, and Saining Xie. Representation alignment for generation: Training diffusion transformers is easier than you think. arXiv preprint arXiv:2410.06940, 2024.
- [94] Xiang Yue, Yuansheng Ni, Kai Zhang, Tianyu Zheng, Ruoqi Liu, Ge Zhang, Samuel Stevens, Dongfu Jiang, Weiming Ren, Yuxuan Sun, et al. Mmmu: A massive multi-discipline multimodal understanding and reasoning benchmark for expert agi. In Proceedings of the IEEE/CVF Conference on Computer Vision and Pattern Recognition, pages 9556–9567, 2024.
- [95] Xiaohua Zhai, Basil Mustafa, Alexander Kolesnikov, and Lucas Beyer. Sigmoid loss for language image pre-training. In Proceedings of the IEEE/CVF international conference on computer vision, pages 11975–11986, 2023.
- [96] Chunting Zhou, Lili Yu, Arun Babu, Kushal Tirumala, Michihiro Yasunaga, Leonid Shamis, Jacob Kahn, Xuezhe Ma, Luke Zettlemoyer, and Omer Levy. Transfusion: Predict the next token and diffuse images with one multi-modal model. arXiv preprint arXiv:2408.11039, 2024.
- [97] Deyu Zhou, Quan Sun, Yuang Peng, Kun Yan, Runpei Dong, Duomin Wang, Zheng Ge, Nan Duan, Xiangyu Zhang, Lionel M. Ni, and Heung-Yeung Shum. Taming teacher forcing for masked autoregressive video generation, 2025. URL <https://arxiv.org/abs/2501.12389>.
- [98] Yichen Zhu, Minjie Zhu, Ning Liu, Zhicai Ou, Xiaofeng Mou, and Jian Tang. Llava-phi: Efficient multi-modal assistant with small language model. arXiv preprint arXiv:2401.02330, 2024.
- [99] Le Zhuo, Ruoyi Du, Han Xiao, Yangguang Li, Dongyang Liu, Rongjie Huang, Wenze Liu, Lirui Zhao, Fu-Yun Wang, Zhanyu Ma, et al. Lumina-Next: Making Lumina-T2X stronger and faster with Next-DiT. arXiv preprint arXiv:2406.18583, 2024.